Cognitive and Motor Loops of the Human Cerebro-cerebellar System

Juha Salmi[1,2*], Karen Johanne Pallesen[1,3,4*], Tuomas Neuvonen[1,2], Elvira Brattico[1,5], Antti Korvenoja[1,6], Oili Salonen[6], and Synnöve Carlson[1,2,7]

Abstract

■ We applied fMRI and diffusion-weighted MRI to study the segregation of cognitive and motor functions in the human cerebro-cerebellar system. Our fMRI results show that a load increase in a nonverbal auditory working memory task is associated with enhanced brain activity in the parietal, dorsal premotor, and lateral prefrontal cortices and in lobules VII–VIII of the posterior cerebellum, whereas a sensory-motor control task activated the motor/somatosensory, medial prefrontal, and posterior cingulate cortices and lobules V/VI of the anterior cerebellum. The load-dependent activity in the crus I/II had a specific relationship with cognitive performance: This activity correlated negatively with load-dependent increase in RTs. This correlation between brain activity and RTs was not observed in the sensory-motor task in the activated cerebellar regions. Furthermore, probabilistic tractography analysis of the diffusion-weighted MRI data suggests that the tracts between the cerebral and the cerebellar areas exhibiting cognitive load-dependent and sensory-motor activity are mainly projected via separated pontine (feed-forward tracts) and thalamic (feedback tracts) nuclei. The tractography results also indicate that the crus I/II in the posterior cerebellum is linked with the lateral prefrontal areas activated by cognitive load increase, whereas the anterior cerebellar lobe is not. The current results support the view that cognitive and motor functions are segregated in the cerebellum. On the basis of these results and theories of the function of the cerebellum, we suggest that the posterior cerebellar activity during a demanding cognitive task is involved with optimization of the response speed. ■

INTRODUCTION

Traditionally, the cerebellum was mainly related to motor processing (Ito, 2002). However, evidence suggesting that the cerebellum is also involved in cognitive processing is accumulating from multiple lines of research (see review by Ramnani, 2006). fMRI studies in healthy humans suggest that motor and cognitive tasks activate different areas of the cerebellum: Motor tasks such as finger tapping activate the lobules IV–VI in the superior parts of the anterior cerebellum, whereas cognitive tasks such as attention shifting or verbal working memory task elicit activity in the posterior cerebellar hemispheres, mainly in the lobules VIIA (that is divided to the crus I and crus II) and VIIB (Allen, Buxton, Wong, & Courchesne, 1997; Desmond, Gabrieli, Wagner, Ginier, & Glover, 1997). Although several studies have reported cerebellar activity during cognitive tasks (Ramnani, 2006), the role of the cerebellum in cognitive processing is unclear. It has been suggested that cerebellar activity in cognitive tasks may be due to uncontrolled motor processes, such as eye movements (Glickstein & Doron, 2008).

The neural connections between the cerebrum and the cerebellum are also suggestive for the involvement of the cerebellum in cognitive processes. Studies in nonhuman primates show that in addition to the motor cortex, also the prefrontal and posterior parietal cortices (pFC and PPC, respectively) provide prominent inputs to the cerebellum (Schmahmann & Pandya, 1989, 1997a, 1997b; Allen, Gilbert, & Yin, 1978; Brodal, 1978). These feed-forward tracts to the cerebellum are projected via specific pontine nuclei, whereas cerebellar feedback signals are transmitted via the thalamus mainly to the same cerebral areas where the feed-forward projections originate (Clower, West, Lynch, & Strick, 2001; Middleton & Strick, 2001; Hoover & Strick, 1999; Lynch, Hoover, & Strick, 1994). Findings in nonhuman primates also suggest that the crus II (in the posterior cerebellar lobe) and Brodmann's area (BA) 46 of pFC and the lobules IV–VI (in the anterior cerebellar lobe) and primary motor cortex (M1) form reciprocal closed loops (Kelly & Strick, 2003).

The tracts between the human cerebellum and the cerebral cortex can be studied with diffusion-weighted MRI (DW-MRI; Jissendi, Baudry, & Balériaux, 2008; Habas & Cabanis, 2007; Ramnani et al., 2006). In line with findings of earlier nonhuman primate studies, these studies have

[1]University of Helsinki, [2]Helsinki University of Technology, [3]Aarhus University, Denmark, [4]Copenhagen University, [5]University of Jyväskylä, Finland, [6]Medical Imaging Center, Helsinki University Central Hospital, [7]University of Tampere
*J. S. and K. J. P. contributed equally on this work.

suggested tracts between the pFC, M1, and PPC and the cerebellum (Jissendi et al., 2008; Ramnani et al., 2006). However, studies in humans have not segregated the "motor" and "cognitive" tracts of the cerebro-cerebellar system. It is also unclear how cerebellar activity that is engaged in cognitive and motor processing is related to performance. Here we used fMRI during tasks that require working memory and a sensory-motor control task to investigate the role of the cerebellum in cognitive and motor processing. We hypothesized that an increase of working memory load would activate areas in the cerebellar lobules VII–VIII, and the sensory-motor task would activate areas in the cerebellar lobules IV–VI. We correlated the observed brain activity with measures of task performance to investigate the association between the cerebellar activity and the task performance. Finally, we collected DW-MRI data to examine feed-forward and feedback tracts between the activated cerebellar areas and the cerebrum.

METHODS

Subjects

Ten healthy right-handed subjects (five women; 22–31 years old, mean age = 25 years) participated in the fMRI experiment. Two of the fMRI subjects (one woman, ages 29 and 28 years) and eight additional subjects (one woman; 23–38 years old, mean age = 28 years) participated in the DW-MRI experiment. All subjects gave a written informed consent before testing in accordance with the experimental protocol approved by the Ethical Committee of the Hospital District of Helsinki and Uusimaa.

The fMRI data are part of a project that also includes a group of professional musicians to investigate the influence of musical expertise on working memory performance and brain responses. The working-memory-related decreases in brain activity have been described in the current group of fMRI subjects in a previous study (Pallesen, Brattico, Bailey, Korvenoja, & Gjedde, 2009).

Stimuli

The stimuli were nine sound combinations (chords) belonging to three different chord categories according to the Western tonal music theory ("major," "minor," and "dissonant"), each spanning three frequency levels separated by an octave. Each chord was produced with the grand-piano timbre of the Roland Sound Canvas SC-50 synthesizer with built-in samples and played using the ENCORE software. The chords were then edited by Cool-Edit and SoundForge programs to balance them with respect to loudness level and duration (870 msec). The major chords transposed over three octave levels consisted of the pitches A, C#, E, A, and C#. Consequently, the major chord was characterized mostly by consonant intervals. The three minor chords played at three octave levels consisted of A, C, E, A, and C, thus including the minor third interval. The three dissonant chords, also played at three octave levels, consisted of A, Bb, G, Ab, and C, thus including a minor second (the interval regarded as the most dissonant one in the Western music theory) and several other dissonant intervals. The sounds were presented via headphones (Commander XG, Resonance Technology Inc., Northridge, CA) through earplugs. The sounds were played at an intensity of approximately 80 dB, individually adjusted so that subjects could clearly hear the sounds and did not feel any discomfort. The sounds were presented with an offset-to-onset interval of 2790 msec. During all tasks, the subjects were asked to visually fixate on a fixation cross presented at the center of a screen that was reflected in a mirror placed on the head coil. By using tasks that do not require eye movements or speech, we minimized the involvement of uncontrolled motor-related processes in the working memory tasks.

Procedure

The subjects pressed one of two buttons in response to each sound. In the one-back task, subjects pressed the left button when the sound was the same as the previous one (one-back target) and in the two-back task when it was the same as the one two sounds back (two-back target). If the sounds were different, they pressed the right button (non-target). In the sensory-motor task, subjects pressed the right button in response to each sound. The sensory-motor task used the same auditory stimuli as the *n*-back tasks (Pallesen et al., 2005, 2009). The two-back and one-back tasks both require stimulus comparison and response selection processes, and they differ with respect to the cognitive load required for memory maintenance and comparison of the sounds in mind. A comparison between the two tasks therefore retains the specific effect of cognitive load while subtracting the effects of sensory and motor processing as both tasks involve similar stimulation and motor responses.

Each subject practiced the task before going to the scanner. During the fMRI measurement, the subject was in the supine position in the scanner, and the head was propped with a moldable vacuum cushion to minimize motion during the experiment. Each block began with a 4-sec presented written instruction (projected centrally on a mirror) indicating the task condition. The duration of each task block was 73.2 sec (containing 20 trials) followed by an 18.3-sec period during which the fixation cross was presented with no sounds. After half of the blocks, there was a 2-min break during which scanning continued, and the subject was instructed to rest until the beginning of the second half of the experiment was announced by a short sound. Twelve blocks for each task condition (one-back, two-back, and a sensory-motor task) were presented in a staircase order (e.g., sensory-motor, one-back, two-back, two-back, one-back, sensory-motor, etc.). After the fMRI experiment, each subject filled in a questionnaire about the experienced difficulty of the tasks, used strategy (auditory

rehearsal, verbal rehearsal, visual imagery, somatosensory imagery, movement, no-strategy), alertness during the experiment, and emotional connotations of the stimuli (Pallesen et al., 2005, 2009).

MRI Data Acquisition

Functional brain imaging was carried out with a 1.5-T Siemens Sonata MRI scanner (Erlangen, Germany) in the Helsinki Medical Imaging Center. The imaging area (covering the whole brain) consisted of 36 functional gradient-echo-planar axial slices (thickness = 4 mm, no gaps, matrix = 64 × 64, echo time [TE] = 40 msec, repetition time [TR] = 3660 msec, field of view = 224 mm, flip angle = 90°). To assure optimal perception of the sounds, we interleaved stimulus presentation with image acquisition. A single functional volume was acquired in 2790 msec, introducing a period of 870 msec with no gradient pulse noise, during which the stimuli were presented. A total of 896 functional volumes were acquired for each subject. Thus, fMRI data acquisition lasted for ca. 54 min. In addition, a T1-weighted (magnetization prepared rapid gradient-echo; MPRAGE) volume was acquired for anatomical alignment (176 sagittal slices, thickness = 1.0 mm, no-gaps, matrix = 256 × 256, TE = 3.68 msec, TR = 1900 msec, flip angle = 15°).

DW-MRI was carried out with a 3.0-T GE Signa Excite MRI scanner (GE Medical Systems, USA) in the AMI center using a quadrature eight-channel head coil. The imaging area covering the whole brain consisted of 54 contiguous axial slices (in-plane resolution = 1.875 × 1.875, slice thickness = 3.0 mm, matrix size = 128 × 128, TE = 78.8 msec, TR = 10,000 msec). Diffusion-weighted volumes (b value = 1000 s/mm^2) were acquired using 60 diffusion-sensitizing gradients with directions isotropically distributed on the surface of a unit sphere using an optimal electron repulsion scheme (R. H. Hardin, N. J. A. Sloane, and W. D. Smith, http://www.research.att.com/~njas/electrons/). The diffusion measurement was performed twice, and a total of eight non-diffusion-weighted images were acquired for reference. For anatomical alignment of the DW images, we acquired a T1-weighted volume (inversion recovery prepared spoiled gradient-echo), 162 contiguous axial slices, thickness = 1 mm, in-plane resolution = 0.9375 × 0.9375 mm, matrix size = 256 × 256, TE = 1.9 msec, TR = 9.1 msec, flip angle = 15°. Imaging time for the DW-MRI images and T1-weighted images at 3 T was approximately 40 min.

Behavioral Data Analysis

The button press responses to the chords were accepted as hits when they were correct and when their latency from target onset was less than 2790 msec (i.e., less than the offset-to-onset interval of the sounds). Other button presses were classified as incorrect responses (IRs). RTs and rates of IRs were calculated within a task condition (sensory-motor, one-back, and two-back) with different chord types combined after the reliability analysis had confirmed that the RTs and IRs were consistent (Cronbach's alpha $>.8$) in the different task conditions. The effect of load on task performance was analyzed using a parametric t test. Pearson's correlations were used to examine the association between the task performance measures (RT and IR) and the relative percentage signal change in the BOLD fMRI data.

fMRI Data Analysis

MR image processing was performed using tools developed at the Functional Magnetic Resonance Imaging of the Brain Centre (FMRIB) that are incorporated into FMRIB Software Library (FSL, release 3.2, www.fmrib.ox.ac.uk/fsl; Smith et al., 2004). BET (Smith, 2002) was used for scalp editing of MR images and FLIRT (Jenkinson, Bannister, Brady, & Smith, 2002) for image registration. Functional data analysis was performed with fMRI Expert Analysis Tool software (FEAT, version 5.43). To allow for the initial stabilization of the fMRI signal, we excluded the first five volumes of the experiment from the analysis. The data were motion corrected and spatially smoothed with a Gaussian kernel of 7 mm (FWHM) and high-pass filtered (cutoff 300 sec). Statistical analysis was performed using the FMRIB improved linear model (Woolrich, Ripley, Brady, & Smith, 2001). The hemodynamic response was modeled using a gamma function (mean lag = 6 sec, SD = 3 sec) and its temporal derivative, and the high-pass filtering applied to the model was the same as that applied to the data. To achieve maximal statistical power, we grouped together the blocks with different chord types after the contrasts among the tasks with different chords within a load level had confirmed that there were no significant differences (at thresholds $Z > 3.1$, cluster corrected $p < .01$) in brain activity as a function of chord type. Explanatory variables for the comparison of two-back and one-back tasks were derived from the timing (onset and duration of each block) in these tasks, and the sensory-motor condition served as a baseline in the model. To extract activations in the sensory-motor task, we modelled this condition with a "rest" baseline condition, which included the instruction periods between the blocks and the break between the two sessions. Individual level Z statistic images were obtained by contrasting the activity in the two-back and one-back tasks with each other (load-dependent activations) and the activity in the sensory-motor task with rest (sensory-motor activations). For single subject load-dependent activations, we used a cluster threshold of $Z > 2.0$ and a cluster-corrected significance threshold of $p < .05$ (corrected for multiple comparisons). For group analyses, we transformed Z statistic images for each subject into standard space (MNI152; Montreal Neurological Institute). The group analyses were performed using FMRIB's local analysis of mixed effects (a cluster threshold of $Z > 3.1$ and a cluster-corrected significance threshold of $p < .01$; Beckmann,

Jenkinson, & Smith, 2003). Because the sensory-motor task had a very low cognitive demand (to minimize the activity of the cognitive load-dependent areas), a lower threshold was used to reveal related brain activity (a cluster threshold of $Z > 2.5$, uncorrected for a cluster significance threshold; Table 1).

DW-MRI Data Analysis

Diffusion-weighted images were corrected for bulk motion and eddy currents using the FLIRT tool (Jenkinson et al., 2002). Nonbrain voxels were removed using BET (Smith, 2002) on a non-diffusion-weighted volume. A coregistration of diffusion-weighted images and anatomical images was obtained using FLIRT with six or seven degrees of freedom and a correlation-ratio-based cost function. The diffusion-weighted and anatomical images were coregistered with the MNI152 average template using FLIRT with 12 degrees of freedom and a correlation-ratio-based cost function. Affine transformation matrices were obtained for each transformation.

Probabilistic tractography was performed with FMRIB diffusion toolkit (Behrens, Woolrich, et al., 2003). Probabilistic tractography algorithm implemented in FMRIB diffusion toolkit attempts to take into account uncertainties in the estimate of fiber direction caused by potential mixture of several fibers within a voxel and noise (physiological, thermal, and measurement related). The method

Table 1. Anatomical Label (Based on Center of Mass), MNI coordinates, and *Z* Score of Global Maxima within Activation Clusters of Significant Cognitive Load-dependent ($Z > 3.6$ and Cluster Corrected $p < .01$) and Sensory-motor Activations

Brain Region	*x*	*y*	*Z*	*Z Score*
(A) Cognitive Load Increase (Two-back vs. One-back)				
Left thalamus	−14	−6	12	7.6
Left middle frontal gyrus (lPFC)	−42	50	4	7.4
Right IPL	32	−64	34	7.4
Right cerebellar lobule VIIB	26	−66	−58	7.0
Right cerebellar crus I	42	−56	−36	6.7
Left cerebellar crus I	−22	−82	−28	6.6
Left superior frontal gyrus (dPMC)	−30	−10	46	6.6
Right middle frontal gyrus (lPFC)	36	38	24	6.6
Left IPL	−42	−48	30	6.5
Left SMA	−6	8	56	6.4
Right superior frontal gyrus (dPMC)	24	−8	54	6.1
Left cerebellar lobule VIII	−46	−50	−40	5.8
Precuneus (SPL)	0	−82	40	5.3
(B) Sensory-motor (Sensory-motor vs. Rest)				
Left superior medial frontal cortex	−8	48	32	4.2
Left precentral gyrus (sensory-motor cortex)	−56	−18	50	3.8
Left middle temporal pole	−40	16	−38	3.6
Right middle temporal pole	38	22	−40	3.5
Left precuneus	−4	−56	34	3.4
Left superior temporal gyrus	−48	−6	6	3.2
Left rolandic operculum	−40	−22	24	3.2
Right precentral gyrus (sensory-motor cortex)	54	−6	50	3.2
Right cerebellar lobule V	14	−54	−24	3.1
Left middle frontal gyrus, orbital part	−12	40	−18	3.0

Anatomical labels are based on Tzourio-Mazoyer et al. (2002) automated anatomical labeling map. In brackets, the more detailed anatomical labels that are used in the text.

has the advantage over the diffusion-tensor-based algorithms in that it is suitable for describing the tracts that progress into regions with nearly isotropic diffusion, such as the gray matter (Behrens, Woolrich, et al., 2003), whereas diffusion-tensor-based tracking algorithms can only trace large fiber tracts in the white matter (Conturo et al., 1999). Tractography analyses were performed in the following order: (1) For each subject, we segmented the pons and the thalamus (delineated from other brain structures) by using the structural brain image. FMRIB's integrated registration and segmentation tool (FIRST) was used for automatic segmentation of the thalamus, and the pons was segmented manually by drawing a mask covering the pons. Pons and thalamus masks were used to examine the cerebro-ponto-cerebellar and cerebello-thalamo-cerebral tracts, respectively. (2) Pontine and thalamic regions receiving projections from cerebral and cerebellar regions, respectively, were examined by classifying the relative strength of the connections to these regions (based on the number of tracts that the tractography algorithm generated). (3) In addition, we examined the cerebro-ponto-cerebellar and cerebello-thalamo-cerebral tracts, that is, those fiber tracts that connected the cerebellar starting points and the pons and thalamus, respectively. Each tractography analysis started from the cerebellar activity cluster, as it is much more difficult to segregate the cerebellar tracts from other tracts when the tracing is done starting from the cerebral cortex. This analysis was separately conducted for each starting point (seed) and endpoint pair consisting of a cerebellar seed and a pontine or a thalamic endpoint mask. (4) Finally, an analysis using cerebellar activity clusters as seeds and cerebro-cortical activity clusters as endpoints was conducted to observe whether the cerebro-ponto-cerebellar and cerebello-thalamo-cerebral tracts connected the activated cerebellar and cerebral areas.

The following analysis parameters were used for iteration of the tracts: step length = 0.5 mm; number of steps = 2000; number of pathways = 5000; and curvature threshold = 0.2 (corresponds approximately to a minimum angle of ±80°). A voxel connectivity threshold value of 50 was applied to the individual level tractography analyses (this threshold represents the number of streamlines passing through the voxel and the seed region). Group images were obtained by adding together the tracts for each individual subject in the MNI space. When investigating the relative strength of connections to and from the pons and the thalamus, we aimed to reveal the pontine and thalamic regions that have the highest probability to be endpoints of the cerebro-cerebellar and cerebello-cerebral tracts. Therefore, in these analyses, thresholding was conducted with a value of 300 for the ipsilateral tracts and 600 for the contralateral tracts. For tracing the tracts between the crus I/II and the pons, we used an even higher threshold (3000 for the ipsilateral tracts and 4500 for the contralateral tracts) because the number of the observed tracts is affected by the size of the seed region and by the distance between the seed and the endpoint regions (Behrens, Woolrich, et al., 2003). Higher threshold values for the contralateral tracts than for the ipsilateral tracts were used because tracing of the crossing fibers more easily gives false-positive results (Jones, 2008). To exclude false-positive tracts, we selected the threshold values for the contralateral tracts on the basis of current knowledge about the contralateral tracts between the cerebellum and the pons (Brodal, 1979) or the thalamus (Middleton & Strick, 2000) and on the pattern of the tractography results of the ipsilateral tracts (the pontine and thalamic nuclei through which they project).

Correlation between Brain Activity and Task Performance

The activated cerebellar areas and the activated cerebral areas showing tracts to the cerebellum (superior parietal lobule [SPL], dorsal premotor cortex [dPMC], anterior pFC [aPFC], and crus I/II in the posterior cerebellum) were identified in the high-resolution anatomical images of individual subjects, and the corresponding ROIs were defined in the space of functional images to test whether the activity within these areas correlated with RT and IR. To exclude effects of intersubject variability on the location of the activated areas, we defined ROIs for determining percentage signal changes in different brain structures on the basis of the peak of activity in individual subjects within the respective anatomical areas. The size of the ROIs was 5 × 5 × 5 voxels in functional space. Before conducting correlation analysis, the load effect on the percentage of signal change was statistically tested for each ROI. SPL, dPMC, aPFC, and crus I/II ROIs showed bilaterally a significant ($p < .05$) load effect.

RESULTS

Task Performance

The load increase (sensory-motor–one-back–two-back) resulted in longer RTs and higher IRs (Figure 1). In the two-back and one-back tasks, RTs were longer ($t = 8.6$, $p < .001$ and $t = 6.0$, $p < .001$, respectively) and IRs higher ($t = 4.5$, $p < .01$ and $t = 2.9$, $p < .05$, respectively) than that in the sensory-motor task. In the two-back tasks, RTs were longer ($t = 6.1$, $p < .001$) and IRs higher ($t = 3.4$, $p < .01$) than that in the one-back tasks (Figure 1). In the sensory-motor tasks, the averaged RT was 613 msec (*SEM* = 63 msec) and IR 1% (*SEM* = 0.8%).

fMRI Results

Load-dependent activity increases (two-back vs. one-back) were observed in all subjects in the SPL and inferior parietal lobule (IPL), dPMC, pFC (covering parts of the superior, middle, and inferior frontal gyri), and posterior cerebellum. The responses were bilateral in all 10 subjects in

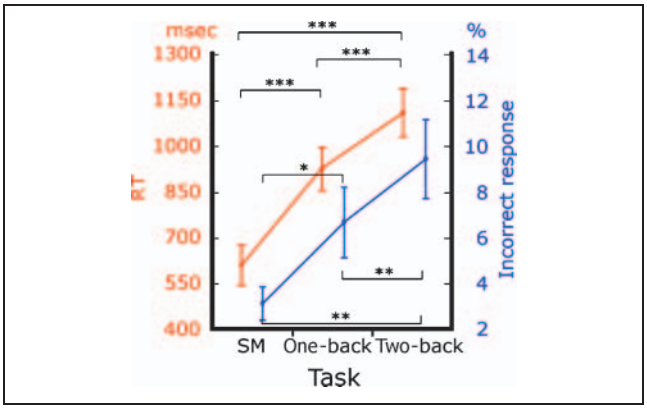

Figure 1. Task performance. Cognitive load-increase resulted in longer RTs and higher rates of IRs. SM = sensory-motor task. $*p < .05$, $**p < .01$, $***p < .001$.

the SPL and IPL, dPMC, and pFC ($Z > 2.0$, cluster corrected $p < .05$). The right posterior cerebellum was activated in all subjects, whereas the left posterior cerebellum was activated in eight subjects. Thus, increased cognitive load led to increased load-dependent activity in a similar brain network in all subjects. The across-subjects two-back versus one-back contrast showed bilateral responses in the intraparietal sulcus (IPS)/SPL, dPMC, pre-SMA, lateral pFC (lPFC, corresponding approximately to BAs 10, 11, and 46/47), BG, and crus I/II of the posterior cerebellum (Figure 2). Moreover, unilateral activity was observed in the right lobule VIIB and left lobule VIII of the cerebellum (Figure 2; Schmahmann, Doyon, Toga, Petrides, & Evans, 2000). The across-subjects two-back versus sensory-motor task contrast showed activity in a mainly similar cerebro-cerebellar network than the one observed for the across-subjects two-back versus one-back task (see Supplementary Figure).

The contrast between the sensory-motor task and the rest periods revealed activity ($Z > 2.5$, uncorrected) in the bilateral motor/somatosensory cortex (MC/SC), medial pFC, superior temporal gyrus, precuneus/posterior cingulate gyrus, and lobules V/VI of the right anterior cerebellum, as revealed by across subjects analysis (Figure 2).

Correlation between Brain Activity and Performance

To test whether the load-dependent brain activity in different areas correlated with RT and IR, we defined a number of ROIs on the basis of the activation clusters of the fMRI study. Between-subjects analysis showed a negative correlation between the load-dependent change in the cerebellar activity and RT (Figure 3). Thus, the greater the increase in crus I/II activity the smaller the increase in RTs. In two-back versus one-back tasks, the correlation between the percent signal change in the left crus I/II and RT was $r = -.735$, $p < .05$, and the percent signal change in the right crus I/II and RT $r = -.760$, $p < .05$. In two-back versus sensory-motor tasks, the percent signal change/RT correlation was $r = -.540$, $p = .107$ in the left crus I/II and $r = -.847$, $p < .001$ in the right crus I/II, and in the one-back versus sensory-motor tasks the percent signal change/RT correlation was $r = -.417$ in the left crus I/II and $r = -.095$ in the right crus I/II. To see whether this correlation between cerebellar activity and task performance is specific for load-dependent activations in the crus I/II, we correlated the activity in the anterior cerebellar (lobule V/VI) ROI with task performance during two-back versus one-back tasks and during sensory-motor task. Neither of these

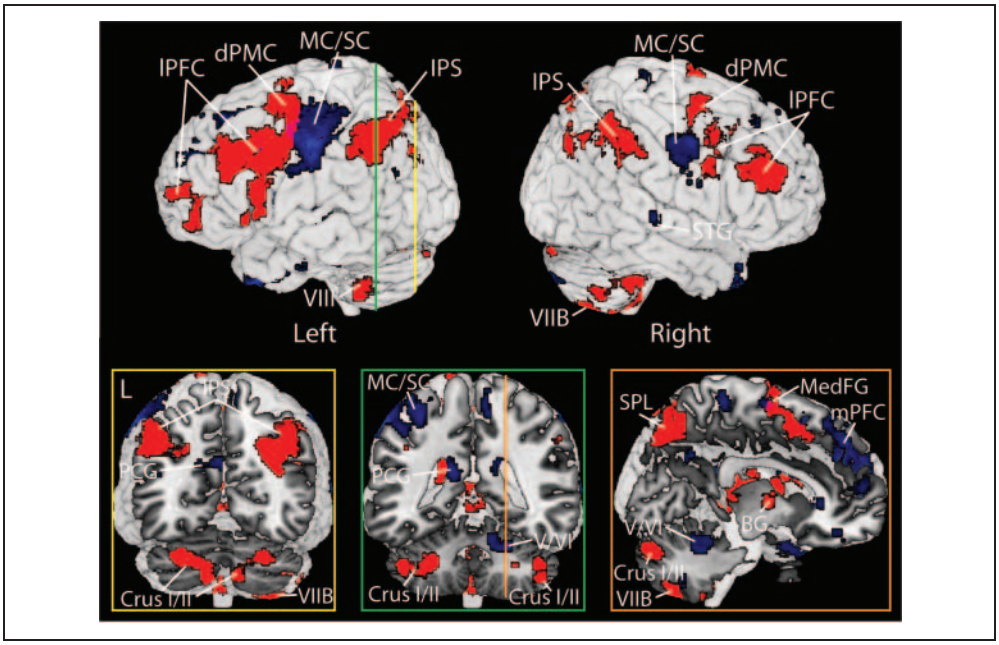

Figure 2. The load-dependent (red clusters, two-back vs. one-back, $Z > 3.1$, cluster corrected $p < .01$) and sensory-motor (blue clusters, sensory-motor task vs. rest, $Z > 2.5$, uncorrected) cerebro-cerebellar activity networks across all subjects ($N = 10$, the reference image is the MNI single subject "Colin" brain; Montreal Neurological Institute). Color-coded vertical lines mark the level of the sections of the images at the bottom. lPFC = lateral pFC; dPMC = dorsal premotor cortex; MC/SC = motor/somatosensory cortex; IPS = intraparietal sulcus; STG = superior temporal gyrus; PCG = posterior cingulate gyrus; mPFC = medial pFC; SPL = superior parietal lobule; BG = basal ganglia; MedFG = medial frontal gyrus; L = left.

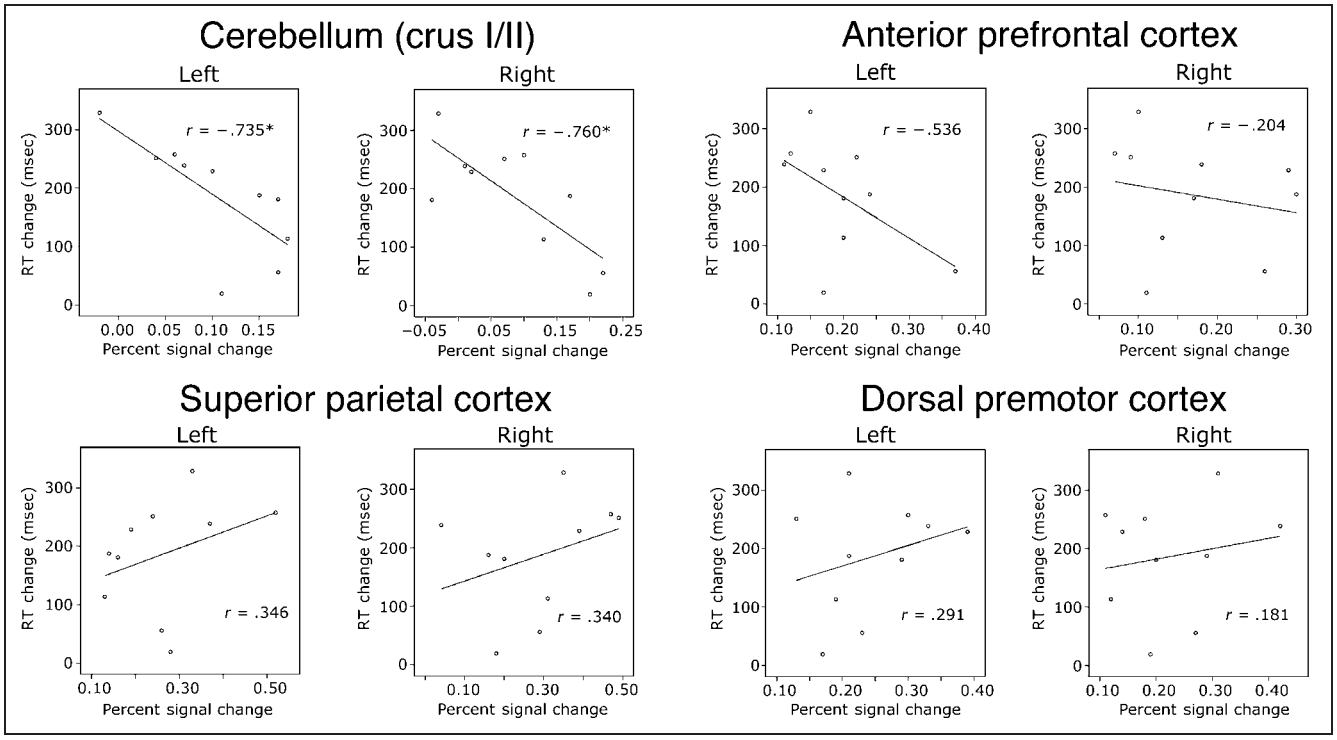

Figure 3. Correlation between the RT and the percentage of signal change in two-back versus one-back tasks in the cerebellum (crus I/II), anterior prefrontal, superior parietal, and dorsal premotor cortices bilaterally (left, right). There was a negative correlation between the RT and the activity in the crus I/II of the cerebellum. $*p < .05$.

conditions showed significant correlations for the RT. Although the correlation between the load-dependent (two-back vs. one-back) percent signal change and RT was not statistically significant in other ROIs (see Figure 3), it should be noted that the tendency of the association of the activity and RT in the aPFC (major target of the posterior cerebellar output; Middleton & Strick, 1994, 2001) was in the same direction as in the crus I/II, whereas in the SPL and dPMC (key input areas of the posterior cerebellum; Schmahmann & Pandya, 1989; Allen et al., 1978; Brodal, 1978) it was in the opposite direction (Figure 3). The IR did not correlate with the load-dependent or sensory-motor activity in any ROI.

Tractography Results

Probabilistic tractography analysis of the DW-MRI data was conducted to examine the tracts between the cerebral and the cerebellar areas that were activated in the fMRI study. Cerebro-ponto-cerebellar and cerebello-thalamo-cerebral tracts were segregated on the basis of the anatomy of these tracts in nonhuman primates (see, Kelly & Strick, 2003; Clower et al., 2001; Middleton & Strick, 2001; Hoover & Strick, 1999; Schmahmann & Pandya, 1989, 1997a, 1997b; Lynch et al., 1994; Allen et al., 1978; Brodal, 1978). To examine the tracts from the cerebrum via pons to the cerebellum, we first determined the relative strength of the tracts between the activated cerebellar areas and the pons. This analysis suggested that the tracts to the cerebellar areas that were activated by cognitive load, especially the crus I/II, project mainly via rostral areas of the basilar pons (Figure 4A), whereas the tracts to the lobule V/VI that showed sensory-motor activity project mainly via more caudal nuclei of the pons (Figure 4A). Thus, our results suggest that cerebro-ponto-cerebellar tracts of the cerebellar areas that were activated by cognitive load and sensory-motor task are projected through different areas of the pons. Further analysis also suggested that the tracts to the other cerebellar areas that were activated by cognitive load (lobules VIIB and VIII) are projected via rostral areas of the pons. On the basis of these results, tracts to the lobule VIII are projected via the lateral surface of the pons, whereas tracts to the lobule VIIB are projected via basal structures of the pons.

After determining the subareas of the pons that have the highest probability of connectivity to the cerebellum, we examined which cerebral areas are linked with the activated cerebellar areas via pons (Figure 5A). Probabilistic tractography using the crus I/II as a seed region showed tracts that linked the anterior pFC (aPFC), dPMC, M1, SC, and SPL with the cerebellum. The lobule VIIB seed showed tracts with the aPFC, M1, and dPMC. The seed in lobule V/VI area that was activated by the sensory-motor task showed tracts with the M1 and dPMC. Each of the observed pontine bundles projected via the capsula interna, cerebral peduncle, and dentate nucleus. The cerebro-ponto-cerebellar tracts for crus I/II, lobule VIIB, and lobule V/VI seeds were observed in each subject, whereas with these thresholds we did not observe tracts between the lobule VIII and the activated cerebro-cortical regions.

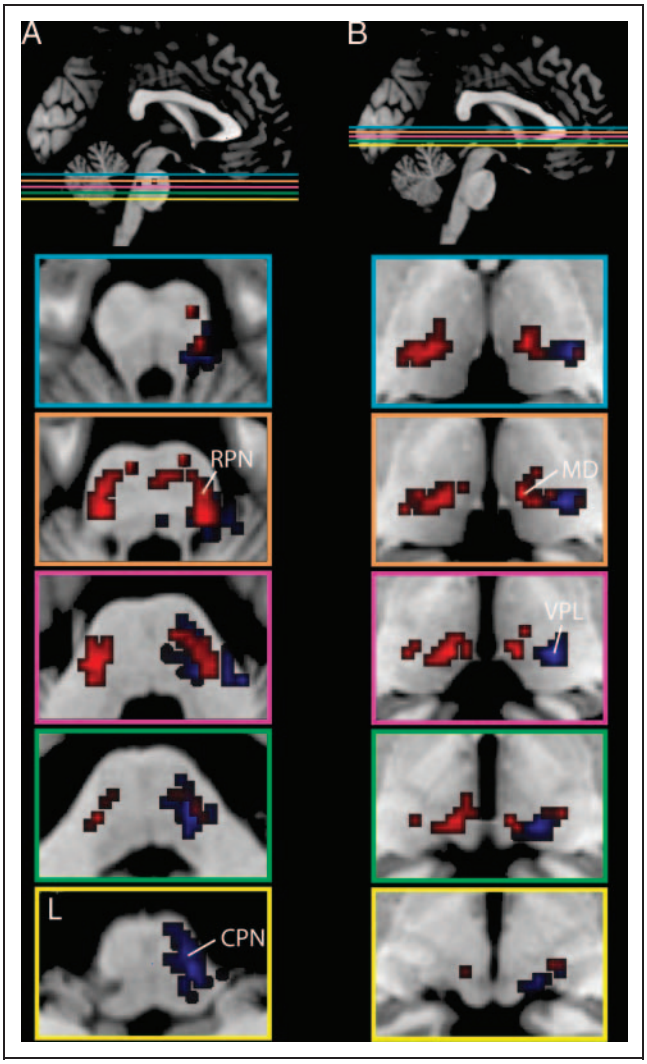

Figure 4. (A) Pontine classification of the cerebro-ponto-cerebellar tracts and (B) thalamic classification of the cerebello-thalamo-cerebral tracts across all subjects ($N = 10$, the reference image is the MNI single subject "Colin" brain; Montreal Neurological Institute). The positions of the slices in the z-axis are indicated by the colored lines in the sagittal sections of the brain (slices are in top-to-bottom order). Endpoints of the tracts traced starting from the right crus I/II activity cluster are shown in red and endpoints of the tracts traced from the right V/VI activity cluster are shown in blue. Areas that are endpoints of both the tracts traced from the crus I/II and lobules V/VI are shown in purple. The figure shows ipsilateral and contralateral tracts traced from the crus I/II activity cluster, and only the ipsilateral tracts traced from the lobule V/VI activity cluster (as we were not able to trace the fibers crossing the hemispheres from the activity cluster in lobules V/VI). Note that different thresholds were used for the ipsilateral and contralateral tracts (see the Methods section). CPN = caudal pontine nuclei; RPN = rostral pontine nuclei; MD = mediodorsal thalamic nuclei; VPL = ventral posterior lateral thalamic nuclei; L = left.

Corresponding analyses that were done for the pons were performed for the thalamus to examine the cerebello-thalamo-cerebral tracts. The classification of thalamic regions based on relative strength of connections suggested that the tracts from the activated area in the crus I/II project mainly via the mediodorsal thalamic nuclei. The thalamic voxel with the highest probability of connection (MNI coordinates; $x = 49, y = 52, z = 36$) with the activated area in the crus I/II has the following connectivity probability pattern in the thalamic connectivity atlas (www.fmrib.ox.ac.uk/connect): .73 pFC, .15 PMC, .15 PPC, .03 occipital cortex, and .03 temporal cortex (note that the probabilities in the thalamic connectivity atlas are defined as the fraction of subjects for whom this location has a probability greater than .25 of connections to each cerebro-cortical mask and therefore the probabilities do not sum to 1). Thus, our results suggest that tracts from the crus I/II to the cerebral cortex project mainly to pFC. A seed in an area in lobule VIIB that also showed load-dependent activity had most numerous endpoints in the ventrolateral thalamic nucleus ($x = 36, y = 55, z = 36$), with connectivity probabilities of .18 with the PMC, .09 with the M1, .09 with the sensory cortex, and .09 with the PPC. Activated areas in the lobules V/VI showed tracts mainly with the ventral posterior lateral thalamic nuclei. The thalamus voxel ($x = 35, y = 52, z = 37$) that showed the highest number of tracts with lobules V/VI that was activated by the sensory-motor task had the following connectivity pattern as suggested by thalamic connectivity atlas: PPC 0.75, sensory cortex 0.41, and M1 0.02. Although this voxel showed only minor tracts with the M1, it should be noted that other thalamus voxels (e.g., $x = 35, y = 53, z = 43$) that showed high number of tracts with the lobules V/VI had >.5 connectivity probability with the M1. Tractography analysis using the activated area in the lobule VIIB as a seed suggested minor tracts with the mediodorsal thalamic nuclei, whereas the activated area in the lobule VIII did not show thalamic endpoints.

The crus I/II and lobule VIIB showed tracts via thalamus with widely distributed areas of the cerebral cortex, including pFC, SPL, dPMC, and M1 (Figure 5B). Corresponding analysis using the V/VI activity cluster as a seed, in turn, revealed tracts only with the MC/SC and SPL (Figure 5B). The observed cerebello-thalamo-cerebral tracts projected from the dentate nucleus to the superior cerebellar peduncles and red nucleus. The cerebello-thalamo-cerebral tracts for crus I/II, lobule VIIB, and lobule V/VI seeds were observed in each subject, whereas the tract from the lobule VIII did not reach the cerebral cortex in any subject with these thresholds.

To test whether the cerebellar activity clusters were connected with the activated cerebral areas, we performed probabilistic tractography analysis using the cerebellar activation clusters as seed masks and cerebral activity clusters as endpoint masks for each subject. This analysis suggested that of the activated cerebellar areas, the crus I/II showed the most prominent tracts with the cerebral areas that were activated by cognitive load (lPFC, dPMC, and SPL). More specifically, tracts between the activated areas in the crus I/II and lPFC, dPMC, and SPL were observed in six or seven subjects, whereas tracts between the activated areas in the crus I/II and M1 were observed only in one subject. The activated area in the anterior cerebellar lobules V/VI, in turn, showed most prominent

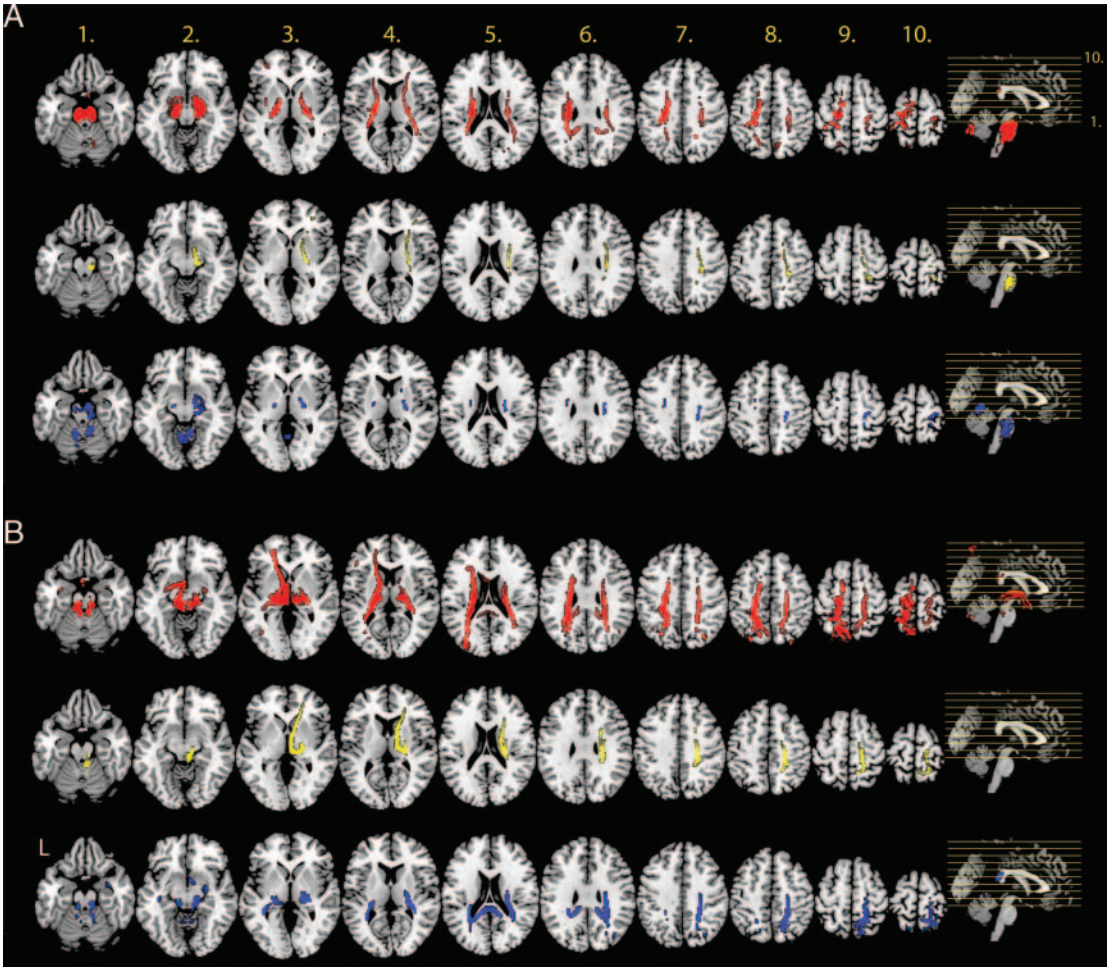

Figure 5. The cerebro-ponto-cerebellar tracts (A) and the cerebello-thalamo-cerebral tracts (B) as revealed by the probabilistic tractography analysis using the activated cerebellar areas as seeds across all subjects (N = 10). Tracts of the crus I/II seed are shown in red, tracts of the lobule VIIB seed are shown in yellow, and tracts of the lobule V/VI seed are shown in blue. L = left.

tracts with the activated area in the SPL (5/10 subjects). Tract between the activated area in the anterior cerebellar lobules V/VI and M1 was observed only in one subject.

DISCUSSION

The present fMRI results show that in addition to the SPL, IPL, dPMC, and lPFC, the cerebellar lobules VII/VIII exhibit cognitive load-dependent activity during short-term memory maintenance and comparison of sounds (Figure 2, red). Both in the cerebral cortex and in the cerebellum, these cognitive load-dependent areas were segregated from the areas that were activated by the sensory-motor task with low cognitive demands (Figure 2, blue). Moreover, there was a cognitive load-dependent negative correlation between the posterior cerebellar (crus I/II) activity and the RT (Figure 3), whereas sensory-motor activation in the cerebellum did not correlate with the RTs in the sensory-motor task. Furthermore, tractography analysis conducted for the DW-MRI data demonstrates that tracts between the cerebral and the cerebellar areas that are activated by the working memory and sensory-motor tasks are mainly segregated in the pons and thalamus (Figure 4) and connect the cerebellum with distinct cerebral areas (Figure 5).

Brain Activity in the Cerebellum and Cerebral Cortex

The present finding of increased pFC, PPC, and posterior cerebellar activity during cognitive load increase is consistent with other studies examining the effects of cognitive load on brain activity (Hayter, Langdon, & Ramnani, 2007; Chen & Desmond, 2005a, 2005b; Kirschen, Chen, Schraedley-Desmond, & Desmond, 2005; Jonides et al., 1997; Schumacher et al., 1996; Zatorre, Evans, & Meyer, 1994). As in previous studies, the cognitive load-dependent cerebellar activity in the present study was observed in crus I/II and lobules VIIB and VIII (Hayter et al., 2007; Chen & Desmond, 2005a, 2005b; Kirschen et al., 2005; Desmond et al., 1997) and the sensory-motor cerebellar activity in the dorsal parts of the anterior cerebellum (Allen et al.,

1997; Desmond et al., 1997). The cerebral areas activated by cognitive load, in turn, differ partially from those found in the previous studies by Desmond et al. (Chen & Desmond, 2005a, 2005b; Kirschen et al., 2005). The differences between the cerebral activations in the present and previous studies are probably due to differences in the tasks. Although the Sternberg working memory tasks used by Chen and Desmond (2005a, 2005b) and Kirschen et al. (2005) mainly measure encoding and maintenance of verbal information that activate the inferior parietal and frontal areas, the *n*-back task also requires manipulation of information in mind which activates more strongly the superior areas of the PPC and pFC including the dPMC and the pre-SMA (e.g., Martinkauppi, Rämä, Aronen, Korvenoja, & Carlson, 2000; Carlson et al., 1998).

Another difference between previous investigations examining the effects of load increase on cerebro-cerebellar activity (Hayter et al., 2007; Chen & Desmond, 2005a, 2005b; Kirschen et al., 2005; Desmond et al., 1997) and the present study is that instead of linguistic stimuli, we used nonlinguistic sounds. Desmond et al. (1997) suggested that load-dependent activity in the cerebellum during verbal working memory reflected facilitation of the phonological loop via computation of the discrepancy between the actual and intended phonological rehearsal signals generated in the cerebral cortex. In the current study, several subjects reported of having used verbal rehearsal to maintain and manipulate information in working memory. However, in addition to load-dependent BOLD responses in triangular and opercular parts of the inferior frontal gyrus associated with subvocal rehearsal (see Chen & Desmond, 2005b), strong activations were present in the dPMC and lPFC. The latter responses, which are also commonly observed in WM studies, gain special interest in the perspective of the tractography analysis performed in the current study. The tractography data yielded no evidence of tracts between the activated cerebellar areas and the abovementioned parts in the inferior frontal cortex associated with subvocal rehearsal. Instead, the observed tracts between the aPFC (approximately BAs 10, 11, and 46/47), the SPL, and the posterior cerebellum indicate the involvement of control processes that are not specific to verbal material. The lPFC is associated with memory maintenance and manipulation of information (Hayter et al., 2007; Carlson et al., 1998) and with several other cognitive processes that are related to executive control (Stuss & Knight, 2002). The SPL is associated with cognitive functions including multimodal attention control (Salmi, Rinne, Degerman, Salonen, & Alho, 2007), spatial working memory (Martinkauppi et al., 2000; Carlson et al., 1998), and motor attention (Rushworth, Nixon, Renowden, Wade, & Passingham, 1997).

Correlation between Posterior Cerebellar Activity and Performance

The cerebellum has been shown to be associated with reaction speed during cognitive processing in previous studies in animals (Nixon & Passingham, 1999), clinical patients (Townsend et al., 1999; Townsend, Harris, & Courchesne, 1996), and healthy human subjects when applying transcranial magnetic stimulation (Desmond, Chen, & Shieh, 2005). Consistently, the present results showed that stronger cognitive-load-related increase in the crus I/II activity during auditory nonverbal working memory tasks was associated with a shorter increase in RT (Figure 3). This association was seen even when the basic level of reactivity (indicated by the sensory-motor task) was taken into account. Other activated regions did not show significant correlations with reaction speed or rate of IRs, although areas of the aPFC that are reciprocally connected with the crus I/II (see also Kelly & Strick, 2003) showed a tendency for a similar negative correlation (this correlation would have been significant if leaving out one outlier, see Figure 3).

Due to its homogenous neuronal organization and connectivity with the cerebral cortex, the cerebellum is regarded as a uniform information processing system that modulates cerebral areas (Ramnani, 2006; Leiner, Leiner, & Dow, 1991). The so-called error correction models suggest that the cerebellum holds an internal simulator that modulates cerebral processing via its feedback projections to the cerebral cortex (Ito, 2006; Marr, 1969). It has been suggested that this modulation of cerebral activity is involved control of shifts of attention by encoding temporally ordered sequences of multidimensional information about external and internal events and by providing short-time scale anticipatory information for the cerebral brain systems (Akshoomoff & Courchesne, 1992). The present results showing cognitive load-dependent posterior cerebellar activations that were associated with shorter RTs are consistent with this suggestion. The lack of association between the RTs in the sensory-motor task and anterior cerebellar activity is possibly due to the easiness of the sensory-motor task. This probably caused also the lower and less significant *Z* values for the sensory-motor task than for the working memory task (see Figure 2).

Cerebro-ponto-cerebellar and Cerebello-thalamo-cerebral Tracts

In keeping with other recent findings (Jissendi et al., 2008; Habas & Cabanis, 2007; Ramnani et al., 2006), our results show that probabilistic tractography analysis is able to trace both the cerebro-ponto-cerebellar (feed-forward) tracts and the cerebello-thalamo-cerebral (feedback) tracts. Our results suggest that tracts connecting the cerebellar areas that were activated by the cognitive load with the cerebral cortex and tracts connecting cerebellar areas that were activated by sensory-motor processing with the cerebral cortex were mainly segregated at the level of pons and thalamus (Figure 4). These findings are in accordance with earlier studies in nonhuman primates (for a review see, Middleton & Strick, 2000; Schmahmann & Pandya, 1997a, 1997b). Findings of the nonhuman primate studies

suggest that the cerebro-pontine projections from different cerebro-cortical areas are projected to specific regions of the pons: pFC projections target mainly rostral areas of the basilar pons, whereas the M1 and PMC projections target more caudal areas of the pons (for a review, see Schmahmann, 1996). These pontine nuclei further project to specific regions of the cerebellum (Brodal, 1979). Brodal (1979) suggested that the lobules V/VI of the cerebellum are linked with the M1 and PMC, whereas the crus I/II is linked mainly with pFC, PMC, and SPL. In accordance with these earlier findings, our results suggest that the cerebro-ponto-cerebellar tracts linking the cerebral cortex with the crus I/II and lobules V/VI of the cerebellum are projected mainly via segregated pontine nuclei. In more detail, the present findings indicate that the cerebro-ponto-cerebellar tracts from pFC, PPC, PMC, and M1 that project to the crus I/II are connected mainly with the rostral nuclei of the basilar pons, whereas the cerebro-ponto-cerebellar tracts from the M1 and PMC to the cerebellar lobules V/VI are connected with more caudal pontine nuclei (see Schmahmann, 1996). In contrast with earlier studies in nonhuman primates (Schmahmann, 1996; Brodal, 1978), we observed only minor ponto-cerebellar projections that projected via the medial pontine nuclei. These projections probably form a relatively smaller portion of the ponto-cerebellar projections in humans than that in nonhuman primates (Ramnani et al., 2006). In addition to a difficulty to detect relatively smaller tract bundles, it is possible that the lack of these tracts in our analysis was due to crossing fibers, close by fibers, or tight bends in the tracts. Finally, we observed only minor overlap in the pons with tracts to areas activated by an increase in cognitive load (the crus I/II) and to areas activated by sensory-motor processes (lobules V/VI; Figure 4A). This overlap may have been due to the common motor tracts.

On the basis of the nonhuman primate studies, cerebello-thalamic tracts from the posterior cerebellar areas involved in cognitive processing target mediodorsal and ventrolateral thalamic nuclei (for a review, see Middleton & Strick, 2000), whereas the anterior cerebellar areas involved in sensory-motor processing target the ventroposterolateral nuclei of the thalamus. Our results are consistent with these earlier findings (Figure 4B). In keeping with the model by Middleton and Strick (2000), the mediodorsal thalamic region that received the most numerous cerebellar tracts shows most prominent connections with pFC according to the thalamic connectivity atlas (www.fmrib.ox.ac.uk/connect). However, our results suggested also other tracts for the crus I/II than pFC tracts (Figure 5). Thus, we did not observe a double dissociation between the "cognitive" and the "motor" loops as suggested by a study in nonhuman primates (Kelly & Strick, 2003). Most likely, the current tractography technique is not as sensitive as the invasive tract tracing techniques in segregating the tracts, especially when they progress into gray matter. It should be noted, however, that also other studies, such as one of the pioneering nonhuman primate studies of the cerebro-cerebellar tracts (Brodal, 1979), suggest that the crus I/II does not form a closed loop with pFC but shows tracts to regions such as the M1, PMC, and PPC. Moreover, as reported in the results, the tract between the activated areas in the crus I/II and M1 was found only in one subject, whereas tracts between the activated areas in the crus I/II and pFC were found in most of the subjects.

Our results further suggest that the tracts of the area in the crus I/II that was activated by cognitive load are connected with the load-dependent cerebral areas. pFC areas that showed tracts with the cerebellum in the present study are mainly in line with the projections reported in the nonhuman primate studies (BAs 8, 9/46, and 10; Kelly & Strick, 2003; Middleton & Strick, 1994, 2000, 2001; Schmahmann & Pandya, 1997a, 1997b). The present results indicate that the human cerebellum is also linked with pFC areas that correspond approximately with BAs 11 and 47, which do not show connections with the cerebellum in nonhuman primates. However, it should be noted that BAs 10, 11, and 47 are next to each other and their correspondence between humans and nonhuman primates is unclear (Petrides & Pandya, 2002). It is possible that BAs 11/47 in nonhuman primates correspond instead to posterior areas of the human IFG (Petrides & Pandya, 2002), which showed no cerebro-cerebellar projections in the present study (see also Schmahmann & Pandya, 1995, 1997a, 1997b; Glickstein, May, & Mercier, 1985; Brodal, 1978).

Tracts between the PMC and the cerebellum were described earlier in nonhuman primates (Allen et al., 1978; Brodal, 1978). Consistent with traditional theories suggesting that the cerebellum is involved in motor processing, Allen et al. (1978) found that the tracts between PMC and SMA and the cerebellum are the most prominent cerebro-cerebellar tracts. Like the cerebellum, the PMC and the pre-SMA are traditionally thought to be involved primarily in motor functions, although several recent studies suggest that they are also involved in cognition (Abe et al., 2007; Hayter et al., 2007; Salmi et al., 2007; Ohbayashi, Ohki, & Miyashita, 2003; Carlson et al., 1998). The present findings of cerebellar and dPMC activity during cognitive processing and the existence of tracts between the activated posterior cerebellar and dPMC areas support this suggestion. Hence, it is possible that the dPMC activity in the present study reflected conversion of the mentally coded serial order of the stimuli into a movement program (Ohbayashi et al., 2003) or binding of the sounds into a meaningful sequence (Abe et al., 2007).

Tracts between the SPL and the cerebellum have been shown earlier in nonhuman primates (Schmahmann & Pandya, 1989; May & Anderson, 1986; Glickstein et al., 1985; Brodal, 1978). Our results in humans are in line with these findings. Most of the observed tracts connected the cerebellum with caudal regions of the SPL, whereas we found only minor projections to the IPL, close to the IPS.

The present study has some methodological restrictions that should be considered when interpreting the results.

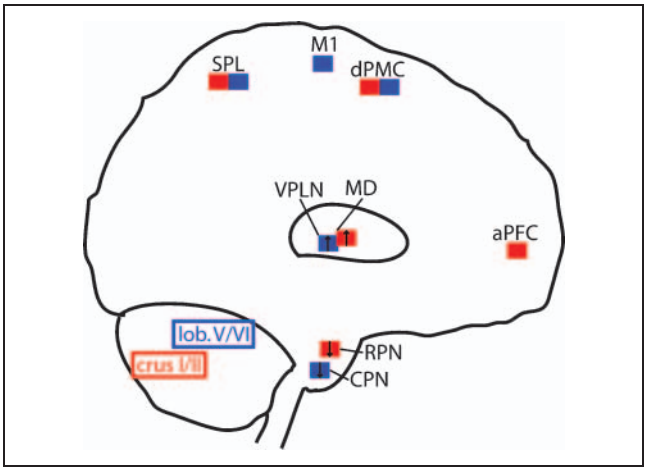

Figure 6. Summary of the observed cerebro-cerebellar network showing (1) the main cerebellar areas involved in cognitive (red, crus I/II) and motor (blue, lobule V/VI) functions, (2) the pontine (feedforward tracts) and thalamic (feedback tracts) regions connecting the cerebellum and cerebral cortex, and (3) the cerebro-cortical regions that originate or target the cerebro-cerebellar tracts. SPL = superior parietal lobule; dPMC = dorsal premotor cortex; VPLN = ventral posterior lateral thalamic nuclei; MD = mediodorsal thalamic nuclei; aPFC = anterior pFC; CPN = caudal pontine nuclei; RPN = rostral pontine nuclei.

First, the employed method is not suitable for comparisons of the proportions of contralateral and ipsilateral tracts because of, for example, the method of the cerebellar seed definition (left and right hemisphere seeds were not comparable in size or shape) and to the bias in tracking the noncrossing fibers. This bias in tracking the noncrossing fibers may also have been the cause for the difficulty to trace the tracts between the activated areas in the cerebellar lobules V/VI and M1. Second, probabilistic tractography analysis does not stop in gray matter (Behrens, Johansen-Berg, et al., 2003). It should be noted that gray matter regions with lower FA values are potential regions where algorithm may show false-positives, especially if several tracts synapse within the same area. Despite of this potential limitation in tracing the multisynaptic tracts, the present study and several other recent studies (Catani et al., 2008; Jissendi et al., 2008; Habas & Cabanis, 2007; Ramnani et al., 2006) suggest that tractography provides results that are in rather well agreement with the findings of invasive studies in nonhuman primates. Third, we had mainly different subjects in the fMRI and DW-MRI studies. Therefore, we had to use ROIs that were defined on the basis of the group analysis results of the fMRI study for the tractography analysis of the DW-MRI study. The advantage of defining the ROIs based on the group analysis results is a better statistical power than individual level analysis (note that in the group analysis, the results do not represent single subjects, thus it would not have made much difference if the subjects in the fMRI and DW-MRI studies would have been the same). Finally, probabilistic tractography does not reveal the direction of the tracts. Therefore, interpretations on the direction of the tracts can only be done on the basis of the existing literature.

Conclusion

The present study combined fMRI, behavioral measures, and DW-MRI to examine the segregation of the cognitive and motor functions in the human cerebro-cerebellar system. Our results suggest that cognitive and motor processes activate segregated areas of the human cerebellum, and these areas have distinct tracts with different connectivity pattern with the cerebral cortex (Figure 6). The cerebellar region crus I/II that was activated by an increase in cognitive load had tracts to the cerebral areas that were similarly activated by cognitive load. Load-dependent activity in the crus I/II also showed a negative correlation with RTs. On the basis of the present results and earlier theories on the functions of the cerebellum (Ito, 2006; Ramnani, 2006), the crus I/II may be involved with optimization of the response speed when the cognitive load increases.

Acknowledgments

Special thanks to Christopher J. Bailey for his help in planning the experiment and fMRI measurements. The authors also thank Jaana Hiltunen and Riitta Hari for technical support in the DW-MRI at the Advanced Magnetic Imaging Centre and Ilkka Linnankoski for his help in revising the language of the manuscript. This study was supported by the Finnish Cultural Foundation, Instrumentarium Science Foundation, Academy of Finland (National Center of Excellence Program), Research Funds of the University of Helsinki, and Finnish Graduate School of Psychology. We gratefully acknowledge the DTI sequence and recon code from Drs Roland Bammer, Michael Moseley, and Gary Glover, supported by the NIH NCRR grant Stanford Center for Advanced Magnetic Resonance Technology, P41 RR09784 (PI: G. Glover).

Reprint requests should be sent to Juha Salmi, Department of Psychology, PO Box 9, FI-00014 University of Helsinki, Finland, or via e-mail: juha.salmi@helsinki.fi.

REFERENCES

Abe, M., Hanakawa, T., Takayama, Y., Kuroki, C., Ogawa, S., & Fukuyama, H. (2007). Functional coupling of human prefrontal and premotor areas during cognitive manipulation. *Journal of Neuroscience, 28,* 3429–3438.

Akshoomoff, N. A., & Courchesne, E. (1992). A new role for the cerebellum in cognitive operations. *Behavioral Neuroscience, 106,* 731–738.

Allen, G., Buxton, R. B., Wong, E. C., & Courchesne, E. (1997). Attentional activation of the cerebellum independent of motor involvement. *Science, 275,* 1940–1943.

Allen, G. I., Gilbert, P. F., & Yin, T. C. (1978). Convergence of cerebral inputs onto dentate neurons in monkey. *Experimental Brain Research, 32,* 151–170.

Beckmann, C. F., Jenkinson, M., & Smith, S. M. (2003). General multilevel linear modeling for group analysis in fMRI. *Neuroimage, 20,* 1052–1063.

Behrens, T. E., Johansen-Berg, H., Woolrich, M. W., Smith, S. M., Wheeler-Kingshott, C. A., Boulby, P. A., et al. (2003). Noninvasive mapping of connections between human thalamus and cortex using diffusion imaging. *Nature Neuroscience, 6,* 750–757.

Behrens, T. E., Woolrich, M. W., Jenkinson, M., Johansen-Berg, H., Nunes, R. G., Clare, S., et al. (2003). Characterization and

propagation of uncertainty in diffusion-weighted MR imaging. *Magnetic Resonance in Medicine, 50,* 1077–1088.
Brodal, P. (1978). The corticopontine projection in the rhesus monkey. Origin and principles of organization. *Brain, 101,* 251–283.
Brodal, P. (1979). The pontocerebellar projection in the rhesus monkey: An experimental study with retrograde axonal transport of horseradish peroxidase. *Neuroscience, 4,* 193–208.
Carlson, S., Martinkauppi, S., Rämä, P., Salli, E., Korvenoja, A., & Aronen, H. J. (1998). Distribution of cortical activation during visuospatial *n*-back tasks as revealed by functional magnetic resonance imaging. *Cerebral Cortex, 8,* 743–752.
Catani, M., Jones, D. K., Daly, E., Embiricos, N., Deeley, Q., Pugliese, L., et al. (2008). Altered cerebellar feedback projections in Asperger syndrome. *Neuroimage, 41,* 1184–1191.
Chen, S. H., & Desmond, J. E. (2005a). Temporal dynamics of cerebro-cerebellar network recruitment during a cognitive task. *Neuropsychologia, 43,* 1227–1237.
Chen, S. H., & Desmond, J. E. (2005b). Cerebrocerebellar networks during articulatory rehearsal and verbal working memory tasks. *Neuroimage, 24,* 332–338.
Clower, D. M., West, R. A., Lynch, J. C., & Strick, P. L. (2001). The inferior parietal lobule is the target of output from the superior colliculus, hippocampus, and cerebellum. *Journal of Neuroscience, 21,* 6283–6291.
Conturo, T. E., Lori, N. F., Cull, T. S., Akbudak, E., Snyder, A. Z., Shimony, J. S., et al. (1999). Tracking neuronal fiber pathways in the living human brain. *Proceedings of the National Academy of Sciences, U.S.A., 31,* 10422–10427.
Desmond, J. E., Chen, S. H., & Shieh, P. B. (2005). Cerebellar transcranial magnetic stimulation impairs verbal working memory. *Annals of Neurology, 58,* 553–560.
Desmond, J. E., Gabrieli, J. D., Wagner, A. D., Ginier, B. L., & Glover, G. H. (1997). Lobular patterns of cerebellar activation in verbal working-memory and finger-tapping tasks as revealed by functional MRI. *Journal of Neuroscience, 17,* 9675–9685.
Glickstein, M., & Doron, K. (2008). Cerebellum: Connections and functions. *Cerebellum, 7,* 589–594.
Glickstein, M., May, J. G., & Mercier, B. E. (1985). Corticopontine projection in the macaque: The distribution of labeled cortical cells after large injections of horseradish peroxidase in the pontine nuclei. *Journal of Computational Neurology, 235,* 343–359.
Habas, C., & Cabanis, E. A. (2007). Anatomical parcellation of the brainstem and cerebellar white matter: A preliminary probabilistic tractography study at 3 T. *Neuroradiology, 49,* 849–863.
Hayter, A. L., Langdon, D. W., & Ramnani, N. (2007). Cerebellar contributions to working memory. *Neuroimage, 36,* 943–954.
Hoover, J. E., & Strick, P. L. (1999). The organization of cerebellar and basal ganglia outputs to primary motor cortex as revealed by retrograde transneuronal transport of herpes simplex virus type 1. *Journal of Neuroscience, 19,* 1446–1463.
Ito, M. (2002). Historical review of the significance of the cerebellum and the role of Purkinje cells in motor learning. *Annals of the New York Academy of Sciences, 978,* 273–288.
Ito, M. (2006). Cerebellar circuitry as a neuronal machine. *Progress in Neurobiology, 78,* 272–303.
Jenkinson, M., Bannister, P. R., Brady, J. M., & Smith, S. M. (2002). Improved optimization for the robust and accurate linear registration and motion correction of brain images. *Neuroimage, 17,* 825–841.
Jissendi, P., Baudry, S., & Balériaux, D. (2008). Diffusion tensor imaging (DTI) and tractography of the cerebellar projections to prefrontal and posterior parietal cortices: A study at 3T. *Journal of Neuroradiology, 35,* 42–50.
Jones, D. K. (2008). Studying connections in the living human brain with diffusion MRI. *Cortex, 44,* 936–952.
Jonides, J., Schumacher, E. H., Smith, E. E., Lauber, E. R., Awh, E., Minoshama, S., et al. (1997). Verbal working memory load affects regional brain activation as measured by PET. *Journal of Cognitive Neuroscience, 9,* 462–475.
Kelly, R. M., & Strick, P. L. (2003). Cerebellar loops with motor cortex and prefrontal cortex of a nonhuman primate. *Journal of Neuroscience, 10,* 8432–8444.
Kirschen, M. P., Chen, S. H., Schraedley-Desmond, P., & Desmond, J. E. (2005). Load- and practice-dependent increases in cerebro-cerebellar activation in verbal working memory: An fMRI study. *Neuroimage, 24,* 462–472.
Leiner, H. C., Leiner, A. L., & Dow, R. S. (1991). The human cerebro-cerebellar system: Its computing, cognitive, and language skills. *Behavioral Brain Research, 44,* 113–128.
Lynch, J. C., Hoover, J. E., & Strick, P. L. (1994). Input to the primate frontal eye field from the substantia nigra, superior colliculus, and dentate nucleus demonstrated by transneuronal transport. *Experimental Brain Research, 100,* 181–186.
Marr, D. (1969). A theory of cerebellar cortex. *Journal of Physiology, 202,* 437–470.
Martinkauppi, S., Rämä, P., Aronen, H. J., Korvenoja, A., & Carlson, S. (2000). Working memory of auditory localization. *Cerebral Cortex, 10,* 889–898.
May, J. G., & Anderson, R. A. (1986). Different patterns of corticopontine projections from separate cortical fields within the inferior parietal lobule and dorsal prelunate gyrus of the macaque. *Experimental Brain Research, 63,* 265–278.
Middleton, F. A., & Strick, P. L. (1994). Anatomical evidence for cerebellar and basal ganglia involvement in higher cognitive function. *Science, 21,* 458–461.
Middleton, F. A., & Strick, P. L. (2000). Basal ganglia and cerebellar loops: Motor and cognitive circuits. *Brain Research Reviews, 31,* 236–250.
Middleton, F. A., & Strick, P. L. (2001). Cerebellar projections to the prefrontal cortex of the primate. *Journal of Neuroscience, 15,* 700–712.
Nixon, P. D., & Passingham, R. E. (1999). The cerebellum and cognition: Cerebellar lesions do not impair spatial working memory or visual associative learning in monkeys. *European Journal of Neuroscience, 11,* 4070–4080.
Ohbayashi, M., Ohki, K., & Miyashita, Y. (2003). Conversion of working memory to motor sequence in the monkey premotor cortex. *Science, 11,* 233–236.
Pallesen, K. J., Brattico, E., Bailey, C., Korvenoja, A., Koivisto, J., Gjedde, A., et al. (2005). Emotion processing of major, minor, and dissonant chords: A functional magnetic resonance imaging study. *Annals of the New York Academy of Sciences, 1060,* 450–453.
Pallesen, K. J., Brattico, E., Bailey, C. J., Korvenoja, A., & Gjedde, A. (2009). Cognitive and emotional modulation of brain default operation. *Journal of Cognitive Neuroscience, 21,* 1065–1080.
Petrides, M., & Pandya, D. N. (2002). Comparative cytoarchitectonic analysis of the human and the macaque ventrolateral prefrontal cortex and corticocortical connection patterns in the monkey. *European Journal of Neuroscience, 16,* 291–310.
Ramnani, N. (2006). The primate cortico-cerebellar system: Anatomy and function. *Nature Reviews Neuroscience, 7,* 511–522.
Ramnani, N., Behrens, T. E., Johansen-Berg, H., Richter, M. C., Pinsk, M. A., Andersson, J. L., et al. (2006). The evolution of

prefrontal inputs to the cortico-pontine system: Diffusion imaging evidence from macaque monkeys and humans. *Cerebral Cortex, 16,* 811–818.
Rushworth, M. F., Nixon, P. D., Renowden, S., Wade, D. T., & Passingham, R. E. (1997). The left parietal cortex and motor attention. *Neuropsychologia, 35,* 1261–1273.
Salmi, J., Rinne, T., Degerman, A., Salonen, O., & Alho, K. (2007). Orienting and maintenance of attention in audition and vision: Multimodal and modality-specific brain activations. *Brain Structure & Function, 212,* 181–194.
Schmahmann, J. D. (1996). From movement to thought: Anatomic substrates of the cerebellar contribution to cognitive processing. *Human Brain Mapping, 4,* 174–198.
Schmahmann, J. D., Doyon, J., Toga, A. W., Petrides, M., & Evans, A. C. (2000). *MRI atlas of the human cerebellum*. London: Academic Press.
Schmahmann, J. D., & Pandya, D. N. (1989). Anatomical investigation of projections to the basis pontis from posterior parietal association cortices in rhesus monkey. *Journal of Computational Neurology, 289,* 53–73.
Schmahmann, J. D., & Pandya, D. N. (1995). Prefrontal cortex projections to the basilar pons: Implications for the cerebellar contribution to higher function. *Neuroscience Letters, 199,* 175–178.
Schmahmann, J. D., & Pandya, D. N. (1997a). Anatomic organization of the basilar pontine projections from prefrontal cortices in rhesus monkey. *Journal of Neuroscience, 17,* 438–458.
Schmahmann, J. D., & Pandya, D. N. (1997b). The cerebrocerebellar system. *International Reviews in Neurobiology, 41,* 31–60.
Schumacher, E. H., Lauber, E., Awh, E., Jonides, J., Smith, E. E., & Koeppe, R. A. (1996). PET evidence for an amodal verbal working memory system. *Neuroimage, 3,* 79–88.
Smith, S. M. (2002). Fast robust automated brain extraction. *Human Brain Mapping, 17,* 143–155.
Smith, S. M., Jenkinson, M., Woolrich, M. W., Beckmann, C. F., Behrens, T. E., Johansen-Berg, H., et al. (2004). Advances in functional and structural MR image analysis and implementation as FSL. *Neuroimage, 23,* S208–S219.
Stuss, D. T., & Knight, R. T. (2002). *Principles of frontal lobe function*. London: Oxford University Press.
Townsend, J., Courchesne, E., Covington, J., Westerfield, M., Harris, N. S., Lyden, P., et al. (1999). Spatial attention deficits in patients with acquired or developmental cerebellar abnormality. *Journal of Neuroscience, 19,* 5632–5643.
Townsend, J., Harris, N. S., & Courchesne, E. (1996). Visual attention abnormalities in autism: Delayed orienting to location. *Journal of International Neuropsychological Society, 2,* 541–550.
Tzourio-Mazoyer, N., Landeau, B., Papathanassiou, D., Crivello, F., Etard, O., Delcroix, N., et al. (2002). Automated anatomical labeling of activations in SPM using a macroscopic anatomical parcellation of the MNI MRI single-subject brain. *Neuroimage, 15,* 273–289.
Woolrich, M. W., Ripley, B. D., Brady, M., & Smith, S. M. (2001). Temporal autocorrelation in univariate linear modeling of fMRI data. *Neuroimage, 14,* 1370–1386.
Zatorre, R. J., Evans, A. C., & Meyer, E. (1994). Neural mechanisms underlying melodic perception and memory for pitch. *Journal of Neuroscience, 14,* 1908–1919.